Research Square

Preprints are preliminary reports that have not undergone peer review.
They should not be considered conclusive, used to inform clinical practice,
or referenced by the media as validated information.

The CO-N2 intermolecular potential energy surface revisited

Dariusz Kędziera
Nicolaus Copernicus University
Omar Rodríguez-López
University of Santiago de Compostela
Ad van der Avoird
Radboud University
Berta Fernández
berta.fernandez@usc.es

University of Santiago de Compostela

Research Article

Keywords:

Posted Date: November 24th, 2026

DOI: https://doi.org/10.21203/rs.3.rs-11731413/v1

License: This work is licensed under a Creative Commons Attribution 4.0 International License.
Read Full License

Additional Declarations: No competing interests reported.

The CO-N_2 intermolecular potential energy surface revisited

Dariusz Kędziera[1*†], Omar Rodríguez-López[2†], Ad van der Avoird[3*†], Berta Fernández[2*†]

[1]Department of Materials Chemistry, Adsorption and Catalysis, Nicolaus Copernicus University, Toruń, 87-100, Poland.
[2]Department of Physical Chemistry, University of Santiago de Compostela, Santiago de Compostela, 15782, Spain.
[3]Theoretical Chemistry, Institute for Molecules and Materials, Radboud University, Nijmegen, 6525 AJ, The Netherlands.

*Corresponding author(s). E-mail(s): teodar@umk.pl; A.vanderAvoird@theochem.ru.nl; berta.fernandez@usc.es;
Contributing authors: omar.rodriguez.lopez@usc.es;
†These authors contributed equally to this work.

Abstract

We developed a new *ab initio* ground-state intermolecular potential-energy surface (IPES) for the CO-N_2 complex evaluated very efficiently with the use of the AutoPES program. The global minimum of the potential corresponds to a planar geometry characterized by the center-of-mass distance $R = 4.153$ Å and the angles $\boldsymbol{\theta_1} = 109.9°$ and $\boldsymbol{\theta_2} = 162.2°$ between the CO and N_2 axes and the vector $\boldsymbol{R}$, with a binding energy of $\boldsymbol{D_e = 118.2}$ $\mathbf{cm^{-1}}$. The accuracy of the potential was assessed by calculating the rovibrational energy levels of the complex. The root-mean-square deviations from the experimental values are 0.096 $\mathbf{cm^{-1}}$ for CO-*ortho*N_2 and 0.065 $\mathbf{cm^{-1}}$ for CO-*para*N_2. Additionally we compared the potential to those previously available. The most accurate one is that in [Phys. Chem. Chem. Phys. **20**, 12636, (2018)], obtained from about 10 000 interaction energies calculated with the CCSD(T) method and Dunning's aug-cc-pVQZ basis set extended with midbond functions. The level of agreement with experiment of the rovibrational energy levels calculated with the latter potential was among the best reported in the literature for weakly bound systems, so we took this potential as a reference. The present AutoPES potential has a global minimum close to that of the reference potential, but it was not able to achieve the accuracy of the latter in providing the rovibrational transitions.

Keywords: CO-N_2 complex, AutoPES, intermolecular potential energy surface, rovibrational spectra

1 Introduction

The theoretical study of weakly bound complexes is a challenge. The high accuracy of the experimental results available makes it mandatory to use highly accurate methods accounting for electron-correlation effects together with extended basis sets in order to obtain accurate intermolecular potential energy surfaces (IPESs) and interaction properties for the complexes. Such methodologies are available and have shown to provide results that approach the experimental accuracy, are sometimes able to correct experimental assignments, and predict properties of complexes that have not been experimentally studied (see Refs. [1, 2] and references therein). A drawback of these methods is that they require the *ab initio* evaluation of a considerable amount of interaction energies, which makes them extremely expensive when complexes with more than three intermolecular coordinates have to be investigated. Considering the high cost involved in the evaluation of accurate intermolecular potentials, in recent years large efforts were set on the development of more efficient methods. The fast development of Machine Learning methods clearly helped and considerably pushed these investigations.

A first step in this direction was the development and implementation of the Automatic Generation of Intermolecular Potential Energy Surfaces (AutoPES) code [3, 4]. AutoPES was applied in the construction of a considerable number of intermolecular potentials (see Refs.[5–9] and references therein) and comparison with accurate potentials previously obtained in a fully human-controlled manner has shown that their quality is acceptable. The advantage of these automatic methods is that, on the one hand, they almost completely eliminate human interaction and, on the other hand, provide the potentials much faster than traditional approaches, with reductions from months to days in many cases. The latter benefit is supported by the generation of a significant smaller number of required grid points.

In the present work we constructed a new IPES for the CO-N_2 complex using the AutoPES code and compared it with the *ab initio* ground-state four-dimensional IPES in Ref. [10] fitted to about 10 000 interaction energies calculated with the CCSD(T) method and Dunning's aug-cc-pVQZ basis set further extended with a set of 3s 3p 2d 1f 1g midbond functions. The global minimum in the latter potential occurs for $R = 4.157$ Å, $\theta_1 = 111.3°$, $\theta_2 = 159.7°$, and $\phi_2 = 0°$ (see Sec. 2 and Fig. 1 for the coordinate definition) with an energy of -118.2 cm^{-1}. Rovibrational energies (up to total angular momentum $J = 20$) were computed on this potential with the symmetry-adapted Lanczos algorithm and the RMSE with respect to spectroscopic data was found to be 0.038 cm^{-1}, which confirmed the high accuracy of the potential. This level of agreement is among the best reported in the literature for weakly bound systems and is considerably better than that achieved with previously published potentials. Therefore, the use of this potential as a benchmark is well justified.

Fig. 1: Definition of the intermolecular coordinates $R, \theta_1, \theta_2, \phi_2$.

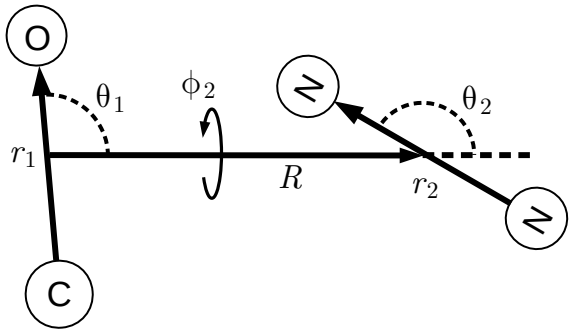

CO-N_2 is a simple weakly bound complex in which the intermolecular forces between two isoelectronic molecules, carbon monoxide (barely polar) and nitrogen (nonpolar), are of significant interest from experimental and theoretical points of view. The system is of great relevance in atmospheric chemistry since N_2 is the primary atmospheric constituent and CO is an important gaseous pollutant. Precise measurements and theoretical predictions of the effects of pressure and temperature on the spectrum of CO perturbed by the dominant atmospheric species, N_2 and O_2, are indispensable for the interpretation of atmospheric absorption data. Ref. [10] includes a extensive review of previous theoretical and experimental studies on the complex. Here we briefly summarize these works (Ref. [10] provides more details) and include the most recent studies carried out after the appearance of Ref. [10].

Spectra of the CO-N_2 complex were first reported in 1996, when infrared (IR) spectra in the region of the CO fundamental band (2146 cm^{-1}) were recorded by Kawashima and Nishizawa [11] and by Xu and McKellar [12]. Pure rotational spectra of CO-N_2 with the ^{14}N and ^{15}N isotopes were observed by Kawashima *et al.* [13]. At the same time, Xu *et al.* [14] studied the microwave and millimeter wave transitions of the *ortho*N_2 states of the complex. In a complementary investigation [15] the rotational and rovibrational spectra of the CO-*para*N_2 complex were measured using a microwave spectrometer in the frequency region from 4 to 26 GHz. The IR spectrum of CO-N_2 was further studied using a pulsed supersonic slit-jet and a rapid-scan tunable diode laser [16].

The first observation of the bend vibration of the CO-N_2 complex in the millimeter wave range from 130 to 155 GHz was reported by Surin *et al.* [17], providing precise information about the vibrational frequency and the rotational constants of the bend excited state. Later on Surin *et al.* [18] carried out new measurements of the CO-N_2 rotational transitions, and in 2015 the studies were completed by reporting new milimeter-wave transitions [19].

In a recent paper [20], an analysis of a new broad-band (2135–2165 cm^{-1}) spectrum of CO-N_2 obtained using a tunable continuous-wave quantum-cascade laser and a pulsed supersonic slit-jet source was presented. Almost 100 new rovibrational levels

were assigned to nine new stacks. However, the authors could not resolve the CO-N_2 structure unambiguously and concluded that dynamical calculations of rotational energy levels were necessary. Also in the experimental studies mentioned above several authors pointed out the necessity of theoretical research as an essential tool in the interpretation of the already available highly accurate experimental data.

The CO-N_2 complex has also been widely investigated from the theoretical point of view. Preliminary work by Fiser *et al.* [21] and by Gribanova *et al.*[22] on a few structures of the complex showed a considerably non-rigid complex, with practically free internal motion of the molecules, and several minima separated by very low barriers.

The first *ab initio* IPES obtained for CO-N_2 was published by Karimi-Jafari *et al.* [23] in 2011. The authors calculated a four-dimensional potential employing the Møller-Plesset fourth-order (MP4) method with a simplified version of the aug-cc-pVQZ basis set of Dunning and coworkers [24]. When compared with results obtained with the CCSD(T) method and the aug-cc-pVTZ basis set extended with a set of 3s 3p 2d 1f midbond functions [25, 26], this potential gave differences of about 5 cm^{-1} in the proximity of the global minimum which rose to 15 cm^{-1} for the linear orientations of the complex. As pointed out in Ref. [10], these large discrepancies might be due to oversimplifications in the theoretical calculations.

In 2018 two studies on the IPES of CO-N_2 have been published [27, 28]. Liu *et al.* [27] obtained a five-dimensional CCSD(T)-F12b/aug-cc-pVQZ IPES which accounted for stretching of the C-O bond. Rovibrational energy levels calculated with the potential resulted in RMSE's with respect to experimental data smaller than 0.068 cm^{-1} in the predicted IR transitions for CO-*ortho*N_2, as well as for CO-*para*N_2. Nonetheless, a considerable number of misprints in the table with the energy levels makes this assertion difficult to confirm. Moreover, the authors did not test the convergence of their method using either larger bases or midbond functions.

The second *ab initio* calculated four-dimensional IPES evaluated with the CCSD(T) correlation method and the aug-cc-pVQZ basis supplemented with a set of 3s 2p 1d midbond functions has been reported by Surin *et al.* [28]. Additionally, they made a new millimeter-wave survey for the CO-N_2 complex in the frequency range of 110–145 GHz. Several transitions not previously observed were detected and assigned. Discrepancies between the calculated and experimental rotational states were observed and a significant number of the detected lines could still not be assigned.

In 2019 Lombardi *et al.* [29] obtained a six-dimensional IPES for the complex using the bond-bond semiempirical method developed by Cappelletti et al [30]. To check the accuracy of the potential the authors applied it in a study of vibration-vibration energy exchange processes of CO in N_2 mixtures. The results were in acceptable agreement with respect to the experimental data for a wide range of temperatures. Considering this, the authors concluded that the potential was suitable for use in dynamics simulations to calculate state-of-the-art rate coefficients.

Recently, Xu and coworkers [31] obtained an accurate 4-dimensional IPES for the complex by taking advantage of the efficiency provided by machine learning methods. The potential is based on 7966 CCSD(T)-F12b/aug-cc-pVQZ interaction energies that were taken as benchmark. The authors compared the potential to the five-dimensional

CCSD(T)-F12b/aug-cc-pVQZ potential evaluated by Liu *et al.* in 2018 [27], and concluded that the agreement between the two PESs was remarkable. Additionally, the effect of reductions in the training set of 50%, 70% and 80% was checked, getting RMSEs lower than 0.5, 1 and 1.5 cm^{-1}, respectively. The above comparison was not performed with respect to the most accurate potential at that time available [10], and from the results in the present paper (shown below) it is clear that for this IPES the agreement for the potential global minimum is better than for the potential in Ref. [27].

In 2023 Sun *et al.* [32] evaluated a new IPES for the CO-N_2 complex and used it in a study of state-to-state rotational energy transfer in collisions. To obtain the CO-N_2 surface, the intermolecular interaction energy was evaluated for 3465 geometries at the CCSD(T) level with an augmented quadruple-zeta basis set. The authors concluded that the potential was in good agreement to the previous one in Ref. [28] and that good agreement was obtained when comparing the theoretical and the experimental results.

This paper is organized as follows: in Sec. 2 we describe the methods and computational details used to develop our potential and to carry out the rovibrational calculations, in Sec. 3 the results are presented and discussed, comparing the performance of the new potential with those previously developed. Section 4 summarizes and provides the conclusions.

2 Computational details

The geometry of the CO-N_2 complex is defined by the following coordinates: the vector $\boldsymbol{R}$ points from the center of mass of CO to that of N_2 and the intermolecular distance R is the length of $\boldsymbol{R}$, θ_1 and θ_2 are the angles between the molecular axes of CO and N_2, respectively, and the vector $\boldsymbol{R}$, and the dihedral angle ϕ_2 is the difference between the azimuthal angles of the CO and N_2 axes. The angles $\theta_1 = 0°$ and $\theta_1 = 180°$ with $\theta_2 = 0°$ (or 180°) correspond to linear CO-N_2 and OC-N_2, respectively, see also Fig. 1. The CO and N_2 bond lengths r_1 and r_2 were fixed at the experimental values: 1.128323 Å and 1.09768 Å [33].

2.1 Construction of the intermolecular potential

The four-dimensional intermolecular potential energy surface of the CO-N_2 complex was generated using the AutoPES package, with both monomers treated as rigid. The short- and intermediate-range interaction energies were calculated at the frozen-core CCSD(T) level, with extrapolation to the complete basis set (CBS) limit using the aug-cc-pVTZ and aug-cc-pVQZ basis sets. The long-range electrostatic, induction, and dispersion contributions were determined using the asymptotic multipole expansion based on density functional theory, as implemented in the SAPT(DFT) package.

To improve the accuracy of the analytical representation of the potential, additional off-nuclear interaction sites were introduced on both monomers. Their positions were systematically selected using a sequential, grid-based optimization procedure. Candidate positions were generated using an in-house Fortran program, with a spacing of 0.01 Å. Since both monomers are linear, all sites were restricted to the molecular

axes to preserve symmetry. Sites were allowed both within and outside the internuclear regions. For N_2, the sites were taken in symmetry-equivalent pairs.

At each optimization step, two independent series of trial calculations were performed concurrently, corresponding to the addition of a new off-nuclear site to CO or a symmetry-related pair of sites to N_2. For each candidate position, the asymptotic parameterization was repeated and the complete intermolecular potential was refitted. The quality of each fit was assessed using the objective function

$$F = \mathrm{RMSE}\big(E_{\mathrm{int}} < E_{\mathrm{min}}/2\big) + \mathrm{RMSE}\big(E_{\mathrm{int}} < 0\big), \tag{1}$$

where E_{min} is the minimum interaction energy in the *ab initio* data set, and both RMSE values are expressed in kcal mol^{-1}. This objective function was adopted as a practical, physically motivated criterion for selecting candidate off-nuclear positions, rather than as a formally derived or demonstrably optimal measure of PES quality. In a weakly bound complex such as CO-N_2 with a highly anisotropic interaction potential, an accurate description of the attractive region, particularly the deeper part of the potential well, is important for representing the configurations sampled by bound rovibrational states. The first RMSE term explicitly favors a close fit in this deeper region, whereas the second term prevents the site selection from focusing exclusively on configurations near the minimum by retaining sensitivity to the entire attractive region. Since points with $E_{\mathrm{int}} < E_{\mathrm{min}}/2$ belong to both subsets, their fitting errors affect both terms and therefore receive additional emphasis in the selection process. The criterion was used only to rank candidate off-nuclear site arrangements; it should not be confused with the energy-dependent weighting scheme used internally to fit the analytical potential in AutoPES. No claim is made that this particular combination of RMSE values is universally optimal or that minimizing it necessarily minimizes errors in the rovibrational energy levels.

The candidate site-positions across both monomers yielding the lowest value of this objective function were selected and kept fixed in all subsequent iterations. To avoid introducing closely spaced interaction sites, candidate positions within approximately 0.1 Å of the selected site were excluded. The procedure was repeated, adding one new off-nuclear site type at each iteration, until a satisfactory fitting accuracy was achieved.

The final representation contains five off-nuclear sites for CO and three symmetry-equivalent pairs for N_2, in addition to the nuclear sites. Their positions and the complete set of potential parameters are provided in the Supplementary Information.

2.2 Calculation of the rovibrational levels

In the calculation of the rovibrational levels of CO-N_2 on the present AutoPES potential we applied a general computational method [34] developed for weakly bound complexes of two nonlinear polyatomic molecules. Such complexes are floppy in general, they often have multiple minima on the IPES with large amplitude internal motions and tunneling between the minima. For all details on the form of the Hamiltonian and the basis in body-fixed (BF) coordinates, etc., we refer to Ref. [34]. As

Table 1: Comparison of the IPES global minimum obtained in different studies of the complex.

IPES	Ref.	R (Å)	$\theta_1(^\circ)$	$\theta_2(^\circ)$	$\phi_2(^\circ)$	Energy (cm^{-1})
4-dim MP4/simplified aug-cc-pVQZ	[23]					-123.1
5-dim CCSD(T)-F12b/aug-cc-pVQZ	[27]	4.155	107.0	166.2	0.0	-117.417
4-dim. CCSD(T)/aug-cc-pVQZ-3s2p1d	[28]	4.159	109.4	162.8	0.0	-117.35
4-dim. ML	[31]	4.163	111.6	160.2	0.0	-118.503
4-dim. AutoPES	this work	4.153	109.9	162.2	0.0	-118.2
4-dim. CCSD(T)/aug-cc-pVQZ-3s3p2d1f1g	[10]	4.157	111.3	159.7	0.0	-118.2

mentioned above, the CO and N_2 monomers were kept rigid; we used rotational constants of 1.92253 cm^{-1} and 1.99824 cm^{-1} [33], respectively. The atomic masses are 14.003074 u for ^{14}N, 12 u for ^{12}C, and 15.994915 u for ^{16}O. The grid for the intermolecular distance R contained 215 equidistant points ranging from $R = 4.5$ to 30 a_0. We used a radial basis of 30 functions contracted in one-dimensional (1D) calculations with the radial kinetic energy and a potential that is a cut of the full four-dimensional potential with the angles fixed at their equilibrium values. This radial basis was variationally optimized by addition of a linear term with a slope of 219 cm^{-1}/a_0, chosen such that the 1D eigenfunctions used in the basis of the full-dimensional calculations minimize the energies of the lowest levels. Here, because the monomers are linear, we use spherical harmonics in the basis instead of the Wigner D-functions [35] used in the general case. The angular basis was truncated to internal rotor quantum numbers $j_{CO} \leq 12$ and $j_{N_2} \leq 11$, with functions of even or odd j_{N_2} for CO-*ortho*N_2 (A-symmetry) and CO-*para*N_2 (B-symmetry), respectively. These values are sufficient to converge the bound levels of the complex to better than 0.0005 cm^{-1}; the energy differences between the levels that are probed spectroscopically are converged even much more accurately. The overall rotation of the dimer was described with Wigner D-functions.

The symmetry group used for this weakly bound complex is not the point group C_s of the equilibrium structure, but the permutation-inversion (PI) or molecular symmetry [36] group. In the present case the group is G_4, generated by the inversion operator and the interchange of the two equivalent nuclei in N_2. The irreducible representations of this symmetry group are A^+, A^- corresponding to the states of CO-*ortho*N_2 with nuclear spin weights of 6, and B^+, B^- corresponding to the states of CO-*para*N_2 with weights 3. The plus and minus signs refer to the parity p under inversion. In our analysis of the rovibrational states we use the spectroscopic parity ϵ, which is related to the inversion parity by $p = \epsilon(-1)^J$, and follow the convention to label states of even/odd spectroscopic parity by e/f. Calculations have been performed for overall angular momentum $J = 0, 1, 2$, for all symmetries.

3 Results and discussion

The new potential is characterized by a global minimum with coordinates $R = 4.153$ Å, $\theta_1 = 109.9°$, $\theta_2 = 162.2°$, $\phi_2 = 0°$, and an energy of -118.2 cm^{-1}. In Table 1 we compare these values to those of the most relevant potentials available. The AutoPES potential minimum is close to that of the CCSD(T)/aug-cc-pVQZ-3s3p2d1f1g potential in Ref. [10]. Figure 2 shows different two-dimensional contour plots of the CO-N_2 IPES. For each plot the remaining two intermolecular coordinates are fixed at the global minimum values and Fig. 3 displays the CO-N_2 IPES in terms of the θ angles for $R = 4.153$Å and $\phi_2 = 0°$. The minimal potential energy configurations are marked with red dots. The nearly barrierless path that allows a large-amplitude motion of the complex can be clearly observed.

Fig. 2: Contour plots of the CO-N_2 IPES (in cm^{-1}). For each plot the remaining two intermolecular coordinates are fixed at the global minimum values.

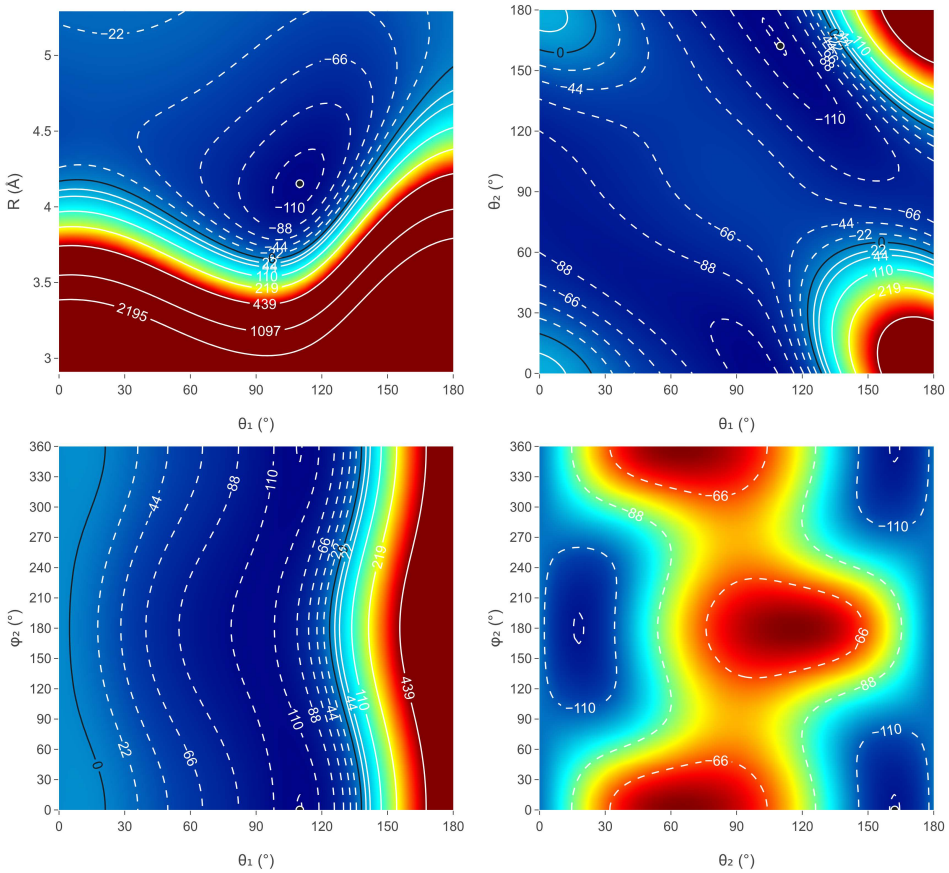

Fig. 3: CO-N_2 IPES for $R = 4.153$ Å and $\phi_2 = 0°$. The minimal potential energy configurations are marked with red dots.

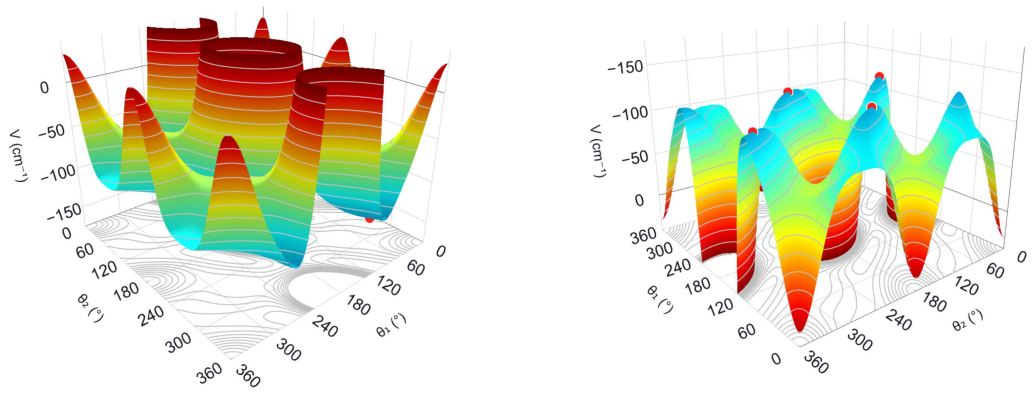

3.1 Quality of the fitted potential and the role of off-nuclear sites

The final analytical representation of the CO-N_2 intermolecular potential contains 15 interaction sites: 7 associated with CO and 8 with N_2. The positions of the off-nuclear sites (5 for CO and 3 pairs for N_2) were determined with the sequential RMSE-based selection procedure described in Sec. 2.1.

The final potential was fitted to 3879 intermolecular interaction energies calculated at the frozen-core CCSD(T)/CBS level. The root-mean-square fitting errors were 0.00102 kcal mol^{-1} (0.36 cm^{-1}) for the 1430 configurations satisfying $E_{\mathrm{int}} < E_{\mathrm{min}}/2$, and 0.00120 kcal mol^{-1} (0.42 cm^{-1}) for the 2811 attractive configurations with negative interaction energies. For the larger set of 3838 configurations with energies below 10 kcal mol^{-1}, the RMSE increased to 0.01179 kcal mol^{-1} (4.12 cm^{-1}). These values describe the accuracy of the analytical representation relative to the *ab initio* energies in the fitting procedure and should not be interpreted as estimates of the accuracy of the underlying electronic-structure calculations.

The relatively small fitting errors in the attractive region indicate that the analytical representation reproduces the calculated interaction energies accurately in the energetically most relevant part of the potential. The final surface also passed the AutoPES hole-scanning procedure, with no unphysical attractive regions identified during this test.

Table 2: Stack labels for CO-*ortho*N_2 and CO-*para*N_2 observed $v_{CO} = 0$ states. The stacks are labeled in the order of increasing energy. The order of stacks for CO-*ortho*N_2 follows that of the $v_{CO} = 1$ state [20].

CO-*ortho*N_2	label	$(j_{CO}, j_{N_2}, K, e/f)$	Ref.
	a	$(0, 0, 0,\ e)$	[18]
	b	$(1, 0, 1,\ e/f)$	[18]
	c	$(1, 0, 0,\ e)$	[18]
	d	$(2, 0, 2,\ e/f)$	
	e	$(2, 0, 1,\ e/f)$	[28]
CO-*para*N_2	label	$(j_{CO}, j_{N_2}, K, e/f)$	
	a	$(0, 1, 0,\ e)$	[18]
	b	$(0, 1, 1,\ e/f)$	[18]
	c	$(1, 1, 1,\ e/f)$	[18]
	d	$(1, 1, 0,\ e)$	[20], [28]
	e	$(1, 1, 2,\ e/f)$	[20], [28]

Table 3: Comparison between the theoretical and the experimental (Obs.) energy levels of CO-*ortho*N_2 (in cm^{-1}). All levels are relative to the ZPE of CO-*ortho*N_2 –76.3164 cm^{-1}. Stack labels are given in Table 2. Calc.1 are the results from the new AutoPES potential, Calc.2 those in Ref. [10], and Calc.3 those in Ref. [28].

		$J = 0,\ A^+(e)$						$J = 0,\ A^-(f)$			
Calc.1	Calc.2	Calc.3	Obs.	K	stack	Calc.1	Calc.2	Calc.3	Obs.	K	stack
0.0000	0.0000	0.0000	0.0000	0	a	16.1596	16.0601			0	
4.7798	4.6863	4.729	4.6663	0	c	23.8801	23.7748			0	
		$J = 1,\ A^+(f)$						$J = 1,\ A^-(e)$			
Calc.1	Calc.2	Calc.3	Obs.	K	stack	Calc.1	Calc.2	Calc.3	Obs.	K	stack
3.7051	3.6333	3.7226	3.6093	1	b	0.1481	0.1480	0.147	0.1486	0	a
8.9843	8.8514	9.016	8.8780	1	e	3.6969	3.6249	3.713	3.6009	1	b
13.6620	13.5885			1		4.9183	4.8246	4.868	4.8057	0	c
15.6384	15.4695			1		8.9755	8.8425	9.007	8.8691	1	e
		$J = 2,\ A^+(e)$						$J = 2,\ A^-(f)$			
Calc.1	Calc.2	Calc.3	Obs.	K	stack	Calc.1	Calc.2	Calc.3	Obs.	K	stack
0.4441	0.4439	0.442	0.4457	0	a	3.9983	3.9262	4.013	3.9034	1	b
3.9737	3.9010	3.988	3.8781	1	b	9.2472	9.1155	9.278	9.1425	1	e
5.1952	5.1013	5.144	5.0845	0	c	10.0017	9.9916			2	
9.2212	9.0893	9.251	9.1161	1	e	11.3927	11.3735			2	

Table 4: Comparison between the theoretical and the experimental (Obs.) energy levels of CO-*para*N_2 (in cm^{-1}). All levels are relative to the ZPE of CO-*para*N_2 –73.5047 cm^{-1}. Stack labels are given in Table 2. Calc.1 are the results from the new AutoPES potential, Calc.2 those in Ref. [10], and Calc.3 those in Ref. [28].

		$J = 0$, $B^+(e)$						$J = 0$, $B^-(f)$			
Calc.1	Calc.2	Calc.3	Obs.	K	stack	Calc.1	Calc.2	Calc.3	Obs.	K	stack
0.0000	0.0000	0.000	0.0000	0	a	6.3659	6.4110			0	
4.4844	4.4205	4.507	4.4955	0	d	15.1034	15.1054			0	
		$J = 1$, $B^+(f)$						$J = 1$, $B^-(e)$			
Calc.1	Calc.2	Calc.3	Obs.	K	stack	Calc.1	Calc.2	Calc.3	Obs.	K	stack
0.0966	0.1979	0.119	0.2324	1	b	0.0396	0.0887	0.054	0.1002	01	a
3.4813	3.4397	3.457	3.4781	1	c	0.1902	0.2420	0.198	0.2655	10	b
6.5060	6.5472			0		3.4816	3.4398	3.485	3.4784	1	c
7.5873	7.4532			1		4.6263	4.5625	4.648	4.6382	0	d
		$J = 2$, $B^+(e)$						$J = 2$, $B^-(f)$			
Calc.1	Calc.2	Calc.3	Obs.	K	stack	Calc.1	Calc.2	Calc.3	Obs.	K	stack
0.2732	0.3200	0.285	0.3360	01	a	0.3955	0.4970	0.417	0.5324	1	b
0.5218	0.5751	0.529	0.5962	10	b	3.7459	3.7040	3.721	3.7445	1	c
3.7468	3.7043	3.722	3.7453	1	c	5.8240	5.8264	5.897	5.8816	2	e
4.9102	4.8465	4.931	4.9234	0	d	6.7856	6.8191			0	
5.8241	5.8265	5.898	5.8818	2	e	7.8886	7.7598			1	

The final potential was constructed using considerably fewer *ab initio* configurations than the approximately 10 000 points employed for the reference potential of Ref. [10]. Although the different electronic-structure protocols prevent a direct comparison of the overall computational cost, this result illustrates the efficiency of the AutoPES sampling strategy.

To further assess the accuracy of the present potential, we calculated the rovibrational energy levels of the CO-N_2 complex for $v_{CO} = 0$. The corresponding stack assignments are provided in Table 2 and the results are summarized in Tables 3 and 4 for CO-*ortho*N_2 and CO-*para*N_2, respectively.

The energy levels obtained using the present AutoPES potential (Calc.1) were compared with those calculated using the potential of Cybulski *et al.* [10] (Calc.2) and those of Surin *et al.* [28] (Calc.3). For CO-*ortho*N_2, the root-mean-square deviation of the calculated energy levels from the experimental values is 0.096 cm^{-1} for the present AutoPES potential, compared with 0.022 cm^{-1} for the reference potential of Ref. [10] and 0.102 cm^{-1} for the potential of Ref. [28]. For CO-*para*N_2, the corresponding deviations are 0.065, 0.047, and 0.053 cm^{-1}, respectively.

These results demonstrate that an accurate reproduction of the global minimum and a small fitting error relative to the underlying *ab initio* data are not sufficient to

guarantee spectroscopic accuracy at the level achieved by the best available potential. Rovibrational energy levels depend on the shape of the potential surface in the configurational regions sampled by the nuclear wavefunctions, including its angular anisotropy and the shallow pathways connecting different molecular orientations. The present comparison does not allow the remaining discrepancies to be attributed uniquely to either the analytical representation or the underlying electronic-structure energies, but it provides a demanding assessment of the overall accuracy of the resulting potential.

4 Summary and concluding remarks

With the use of the AutoPES package we developed a new four-dimensional intermolecular potential energy surface for the CO-N_2 complex. The short- and intermediate-range interaction energies were calculated at the frozen-core CCSD(T) level and extrapolated to the complete basis set limit, while the long-range behavior was described using asymptotic information obtained from SAPT-based calculations. The final analytical potential accurately reproduces the location and depth of the global minimum of the CO-N_2 complex and provides a qualitatively correct description of its shallow and strongly anisotropic interaction energy landscape. However, the rovibrational levels of the complex calculated on this potential reveal somewhat larger deviations from experiment than those obtained with the most accurate reference potential. This demonstrates the importance of spectroscopic benchmarks for assessing the accuracy of intermolecular potentials beyond their equilibrium properties.

The present study also highlights the importance of placing off-nuclear interaction sites in the AutoPES analytical representation. A sequential optimization procedure based on the minimization of fitting errors was employed to optimize the positions of additional interaction sites while preserving molecular symmetry. Although this approach yielded a satisfactory analytical representation, it required repeated parameterizations and intermolecular potential fits for numerous candidate site positions.

AutoPES provides a powerful framework for the automated construction of intermolecular potential energy surfaces. Nevertheless, the optimal placement of off-nuclear sites remains a methodological challenge. A desirable future development would be an automated procedure that determines suitable off-nuclear positions directly from the electronic properties of isolated monomers, rather than through repeated optimization of the final PES fitting error.

For nonlinear molecules, the absence of the axial symmetry constraints imposed in the present CO-N_2 study provides considerably greater freedom in the placement of additional interaction sites. This may offer opportunities for a more accurate representation of the angular dependence of intermolecular interactions. At the same time, the larger search space makes efficient, physically motivated strategies for off-nuclear placement even more important. Such developments could further improve the balance between computational efficiency, automation, and accuracy in the construction of intermolecular potential energy surfaces.

Supplementary information. The Supporting Information is available free of charge. It contains details on the interaction sites and asymptotic site parameters, the analytical potential and the fitted parameters, and the final fitting statistics.

Acknowledgements. We dedicate this work to the memory of our friend and colleague Bogumił Jeziorski. The authors acknowledge funding from the Spanish Agencia Estatal de Investigación (AEI) through the National Project PID2025-173245NB-100 and from the Xunta de Galicia, grant number ED431C 2025/06. We are also grateful for support from the EU Doctoral Network PHYMOL 101073474 (project call reference HORIZON-MSCA-2021-DN-01) and from the COST Action CA21101 "Confined molecular systems: from a new generation of materials to the stars" (COSY) from the COST (European Cooperation in Science and Technology). We thank the CESGA supercomputer center (Spain) for computational resources.

References

[1] Cybulski, H., Fernández, B., Henriksen, C., Felker, P.M.: Ab initio ground state phenylacetylene-argon intermolecular potential energy surface and rovibrational spectrum. J. Chem. Phys. **137**, 074305 (2012)

[2] Munteanu, C.R., Fernández, B.: Accurate intermolecular ground-state potential-energy surfaces of the HCCH–He, Ne, and Ar van der Waals complexes. J. Chem. Phys. **123**, 014309 (2005)

[3] Metz, M., Piszczatowski, K., Szalewicz, K.: Automatic generation of intermolecular potential energy surfaces. J. Chem. Theory Comput. **12**, 5895 (2016)

[4] Metz, M., Szalewicz, K.: Automatic generation of intermolecular potential energy surfaces. J. Chem. Theory Comput. **16**, 2317 (2020)

[5] Tóbiás, R., Fábri, C., Bosquez, M., Kodrycka, M., Patkowski, K., Császár, A.: Rovibrational dynamics of the quasistructural N_2 dimer. Commun. Chem. **8**, 339 (2025)

[6] Vindel-Zandbergen, P., Kędziera, D., Żółtowski, M., J., K., Żuchowski, P., Felker, P.M., Lique, F., Bačić, Z.: H_2O–HCN complex: A new potential energy surface and intermolecular rovibrational states from rigorous quantum calculations. J. Chem. Phys. **159**, 174302 (2023)

[7] Derbali, E., Mehnen, B., Żuchowski, P.S., Kędziera, D., Al-Mogren, M.M., Jaidane, N.-E., Hochlaf, M.: Towards the generation of potential energy surfaces of weakly bound medium-sized molecular systems: the case of benzonitrile–He complex. Phys. Chem. Chem. Phys. **25**, 30198 (2023)

[8] Salem, J., Tóbiás, R., Császár, A.G., Al-Mogren, M.M., Jaidane, N.-E., Hochlaf, M.: Temperature-dependent line-broadening effects in CO_2 caused by Ar. Chem. Phys. Chem. **25**, 202300467 (2024)

[9] Aling, J., Szalewicz, K., van der Avoird, A.: Ammonia dimer: extremely fluxional but still hydrogen bonded. Nature Commun. **13**, 1470 (2022)

[10] Cybulski, H., Henriksen, C., Dawes, R., Wang, X.-G., Bora, N., Avila, G., Carrington, T.J., Fernández, B.: Ab initio study of the CO–N_2 complex: a new highly accurate intermolecular potential energy surface and rovibrational spectrum. Phys. Chem. Chem. Phys. **20**, 12624 (2018)

[11] Kawashima, Y., Nishizawa, K.: Pulsed molecular beam infrared absorption spectroscopy of the N_2-CO complex. Chem. Phys. Lett. **249**, 87 (1996)

[12] Xu, Y., McKellar, A.R.W.: Continuous slit-jet infrared spectrum of the CO-N_2 complex. J. Chem. Phys. **104**, 2488 (1996)

[13] Kawashima, Y., Ohshima, Y., Endo, Y.: Rotational spectrum of the $N_2 \cdots CO$ complex: ortho-N_2 and para-N_2. Chem. Phys. Lett. **315**, 201 (1999)

[14] Xu, Y., Jäger, W., Surin, L.A., Pak, I., Panfilov, L.A., Winnewisser, G.: Microwave and millimeter wave study of ortho-N_2 states of CO–N_2. J. Chem. Phys. **111**, 10476–10483 (1999)

[15] Xu, Y., Jäger, W.: The dynamics of the CO–N_2 interaction: Strong coriolis coupling in CO-paraN_2. J. Chem. Phys. **113**, 514–524 (2000)

[16] Xia, C., McKellar, A.R.W., Xu, Y.: Infrared spectrum of the CO-N_2 van der waals complex: Assignments for CO-*para*N_2 and observation of a bending state for CO-*ortho*N_2. J. Chem. Phys. **113**, 525 (2000)

[17] Surin, L.A., Müller, H.S.P., Alieva, E.V., Dumesh, B.S., Winnewisser, G., Pak, I.: Detection of the bending vibration of the CO-*ortho*N_2 complex. J. Mol. Struct. **612**, 207 (2002)

[18] Surin, L.A., Potapov, A.V., Müller, H.S.P., Panfilov, V.A., Dumesh, B.S., Giesen, T.F., Schlemmer, S.: Millimeter-wave study of the CO-N_2 van der waals complex: new measurements of CO–ortho-N_2 and assignments of new states of CO–para-N_2. J. Mol. Struct. **795**, 198 (2006)

[19] Surin, L.A., Potapov, A., Müller, H.S.P., Schlemmer, S.: A new millimeter-wave observation of the weakly bound CO-N_2 complex. J. Mol. Spectrosc. **307**, 54 (2015)

[20] Rezaei, M., Michaelian, K.H., Moazzen-Ahmadi, N., McKellar, A.R.W.: A new look at the infrared spectrum of the weakly bound CO-N_2 complex. J. Phys. Chem. A **117**, 13752 (2013)

[21] Fišer, J., Polák, R.: An ab initio study of the CO-N_2 complex. Chem. Phys. Lett. **360**, 565 (2002)

[22] Gribanova, T.N., Milov, A.A., Gapurenko, O.A., Starikov, A.G., Gurashvili, V.A., Minyaev, R.M., Minkin, V.I.: Structure and stability of the mixed polymolecular complexes of nitrogen and carbon nonooxide: A quantum chemical study. Russ. J. Gen. Chem. **81**, 807 (2011)

[23] Karimi-Jafari, M.H., Maghari, A., Farjamnia, A.: Intermolecular potential energy surface of the N_2-CO dimer: Ab initio investigation and analytical representation. J. Phys. Chem. A **115**, 1143 (2011)

[24] Dunning, T.H. Jr.: Gaussian basis sets for use in correlated molecular calculations. i. the atoms boron through neon and hydrogen. J. Chem. Phys. **90**, 1007 (1989)

[25] Tao, F.-M., Pan, Y.-K.: Møller–plesset perturbation investigation of the He_2 potential and the role of midbond basis functions. J. Chem. Phys. **97**, 4989 (1992)

[26] Tao, F.-M.: The use of midbond functions for ab initio calculations of the asymmetric potentials of He-Ne and He-Ar. J. Chem. Phys. **98**, 3049 (1993)

[27] Liu, J.-M., Zhai, Y., Zhang, X.-L., Li, H.: Intermolecular configurations dominated by quadrupole-quadrupole electrostatic interactions: explicit correlation treatment of the five-dimensional potential energy surface and infrared spectra for the CO-N_2 complex. Phys. Chem. Chem. Phys. **20**, 2036 (2018)

[28] Surin, L.A., Tarabukin, I.V., Schlemmer, S., Kalugina, Y.N., van der Avoird, A.: Ab initio potential and rotational spectra of the CO-N_2 complex. J. Chem. Phys. **148**, 044313 (2018)

[29] Lombardi, A., Pirani, F., Bartolomei, M., Coletti, C., Laganà, A.: Full dimensional potential energy function and calculation of state-specific properties of the CO+N_2 inelastic processes within an open molecular science cloud perspective. Front. Chem. **7**, 309 (2019)

[30] Cappelletti, D., Pirani, F., Bussery-Honvault, B., Gomez, L., Bartolomei, M.: A bond–bond description of the intermolecular interaction energy: the case of weakly bound N_2–H_2 and N_2–N_2 complexes. Phys. Chem. Chem. Phys. **10**, 4281 (2008)

[31] Xu, S., Li, Y., Wang, D., Fang, C., Luo, C., Deng, J., Hu, L., Li, H., Li, H.: Efficient prediction for high precision CO-N_2 potential energy surface by stacking ensemble DNN. J. Comput. Chem. **43**, 244 (2022)

[32] Sun, Z.-F., A., S.R.J., Hermert M. C., A., v., Suits, A.G., Parker, D.H.: Imaging rotational energy transfer: comparative stereodynamics in CO + N_2 and CO + CO inelastic scattering. Phys. Chem. Chem. Phys. **25**, 17828 (2018)

[33] Huber, K.P., Herzberg, G.: Molecular Spectra and Molecular Structure. IV.

Constants of Diatomic Molecules. van Nostrand Reinhold Company, New York (1979). see *http://webbook.nist.gov*

[34] Groenenboom, G.C., Wormer, P.E.S., van der Avoird, A., Mas, E.M., Bukowski, R., Szalewicz, K.: Water pair potential of near spectroscopic accuracy: Ii. vibration-rotation-tunneling levels of the water dimer. J. Chem. Phys. **113**, 6702–6715 (2000)

[35] Brink, D.M., Satchler, G.R.: Angular Momentum, 3rd edn. Clarendon, Oxford (1993)

[36] Bunker, P.R., Jensen, P.: Molecular Symmetry and Spectroscopy, 2nd edn. NRC Research Press, Ottawa (1998)

Graphical abstract. A new *ab initio* ground-state intermolecular potential-energy surface for the CO-N_2 complex was evaluated in an efficient way using the AutoPES code.

Fig. 4

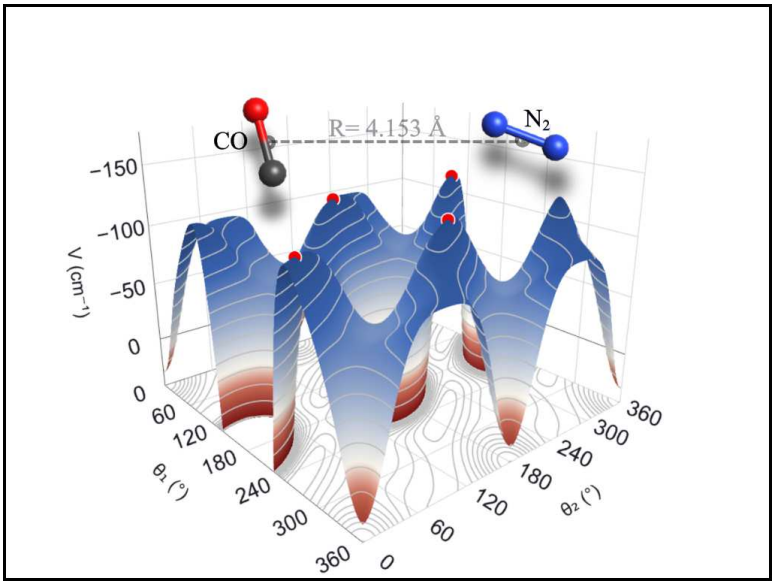

Supplementary Files

This is a list of supplementary files associated with this preprint. Click to download.

- SICON2revisited.pdf